

# Mutex Propagation in Multi-Agent Path Finding for Large Agents

Han Zhang, Yutong Li, Jiaoyang Li, T. K. Satish Kumar, Sven Koenig

University of Southern California

{zhan645, yli81711, jiaoyanl}@usc.edu, tskwork@gmail.com, skoenig@usc.edu

## Abstract

Mutex propagation and its concomitant symmetry-breaking techniques have proven useful in Multi-Agent Path Finding (MAPF) with point agents. In this paper, we show that they can be easily generalized to richer MAPF problems. In particular, we demonstrate their application to MAPF with “Large” Agents (LA-MAPF). Here, agents can occupy multiple points at the same time according to their fixed shapes and sizes. While existing rule-based symmetry-breaking techniques are difficult to generalize from point agents to large agents, mutex-based symmetry-breaking techniques can be generalized easily. In a Conflict-Based Search (CBS) framework for LA-MAPF, we also develop a mutex-based conflict-selection strategy to further enhance the efficiency of the search. Through experiments on various maps, we show that our techniques significantly improve MC-CBS, a state-of-the-art optimal LA-MAPF algorithm, in terms of both success rate and runtime.

## Introduction and Related Work

The Multi-Agent Path-Finding (MAPF) problem is a generalization of the single-agent path-finding problem to multiple agents. Each agent is required to move from a given start vertex to a given goal vertex on a given graph while avoiding collisions with other agents. Solving the MAPF problem optimally is known to be NP-hard for various objective functions (Yu and LaValle 2013; Ma et al. 2016). Although the MAPF problem arises in many real-world application domains (Wurman, D’Andrea, and Mountz 2008; Morris et al. 2016), MAPF research has mostly focused on point agents, i.e., agents that have no shape or size.

MAPF with Large Agents (LA-MAPF) is a generalization of MAPF that bestows shape and size to the agents to make them more realistic. However, generalizing existing algorithmic techniques for MAPF to LA-MAPF can be non-trivial. For example, while Conflict-Based Search (CBS) is designed to solve the MAPF problem, generalizing it to solving the LA-MAPF problem efficiently requires more sophisticated reasoning, as encapsulated in Multi-Constraint CBS (MC-CBS) (Li et al. 2019b).

Another important paradigm for enhancing search in MAPF with point agents is symmetry breaking. Existing

symmetry-breaking techniques fall into two categories: (a) rule-based techniques (Li et al. 2019a, 2020) and (b) mutex-based techniques (Zhang et al. 2020; Walker et al. 2021). However, none of these techniques have been generalized to LA-MAPF. Rule-based techniques are human-generated, handle only limited kinds of symmetries, and are difficult to generalize to LA-MAPF. Mutex-based techniques are derived from constraint propagation and handle more general kinds of symmetries.

In later sections, we describe how mutex propagation and its concomitant symmetry-breaking techniques can be generalized to LA-MAPF. In fact, the generalization makes these techniques applicable to other richer MAPF problems as well. We also develop a mutex-based conflict-selection strategy to further enhance the efficiency of search. In the experimental results, we show that our techniques significantly improve MC-CBS, a state-of-the-art optimal LA-MAPF algorithm, in terms of both success rate and runtime.

## Preliminaries

In this section, we provide background material related to MAPF, LA-MAPF, and CBS.

### MAPF and LA-MAPF

The MAPF problem is defined by an undirected graph  $G = (V, E)$  and a set of  $m$  agents  $\{a_1 \dots a_m\}$ . Each agent  $a_i$  has a start vertex  $s_i \in V$  and a goal vertex  $g_i \in V$ . In each timestep, an agent either moves to a neighboring vertex, waits at its current vertex, or terminates at its goal vertex (that is, does not move anymore). A *path* of an agent is a sequence of actions that leads it from its start vertex to its goal vertex and ends with a terminate action. The *path cost* of a path is the number of timesteps from beginning to termination. A *vertex conflict* happens when two agents stay at the same vertex simultaneously, and an *edge conflict* happens when two agents traverse the same edge in opposite directions simultaneously. A *solution* is a set of conflict-free paths of all agents. In this paper, we focus on minimizing the Sum of path Costs (SoC), that is, the sum of the path costs of the paths of all agents.

LA-MAPF generalizes MAPF to agents with different shapes and sizes. In LA-MAPF,  $G$  is embedded in a  $d$ -dimensional Euclidean space (usually  $d = 2, 3$ ). Each agent has a fixed shape around a *reference point* and can occupy

multiple vertices at the same time. A *vertex conflict* happens when the shapes of two agents overlap at some timestep, and an *edge conflict* happens when the shapes of two agents overlap at some time when they move to their respective next vertices. In this paper, we focus on 2-dimensional grids. However, mutex propagation does not make any assumption of the space embedding of  $G$  and hence can be applied in other settings as well.

## CBS

CBS (Sharon et al. 2015) is an optimal two-level MAPF algorithm. On the high level, CBS performs a best-first search on a *Constraint Tree* (CT). Each CT node contains (1) a set of constraints and (2) a set of paths, one for each agent, that satisfy all these constraints. The cost of a CT node is the SoC of the paths. CBS starts with the root CT node, which has an empty set of constraints and a path for each agent that has the minimum path cost when ignoring conflicts. When expanding a CT node, CBS returns the paths of it as a solution if the paths are conflict-free. Otherwise, CBS picks a conflict to resolve, splits the CT node into two child CT nodes, and adds a constraint to each child CT node to prohibit either one or the other of the two conflicting agents from using the conflicting vertex or edge at the conflicting timestep. For the newly constrained agent in each child CT node, CBS then calls its low level to find an *individual minimum-cost path*, that is, a path that has the minimum cost while satisfying all constraints of the CT node but ignoring conflicts.

**Multi-Decision Diagrams (MDDs):** An MDD (Sharon et al. 2013, 2015)  $MDD_i^l$  for agent  $a_i$  in a CT node is an  $(l + 1)$ -level directed acyclic graph that consists of all paths of cost  $l$  for agent  $a_i$  that satisfy all constraints of the CT node. Cost  $l$  is usually set to the *individual minimum cost* (that is, the cost of the individual minimum-cost path) of  $a_i$  but not necessarily so. Each MDD node  $n$  of  $MDD_i^l$  at level  $t$  correspond to a vertex of agent  $a_i$  at timestep  $t$  in these paths. We use  $n.loc$  and  $n.level$  to denote the corresponding vertex and  $t$ , respectively. Slightly abusing the notation, we use  $n \in MDD_i^l$  to denote that  $n$  is an MDD node of  $MDD_i^l$ . At level 0,  $MDD_i^l$  has a single *source MDD node* corresponding to agent  $a_i$  occupying its start vertex  $s_i$  at timestep 0. At level  $l$ ,  $MDD_i^l$  has a single *sink MDD node* corresponding to agent  $a_i$  occupying its goal vertex  $g_i$  at timestep  $l$ .

**Cardinal Conflicts:** Two agents have a *cardinal conflict* in a CT node iff there does not exist a pair of conflict-free individual minimum-cost paths for both agents (that, by definition, satisfy all constraints of the CT node). That is, the SoC of an optimal solution for the two agents is larger than the SoC of the individual minimum-cost paths of them. CBS cannot resolve all cardinal conflicts efficiently since it needs to check all combinations of paths whose SoC is less than the SoC of an optimal solution, which can necessitate many CT node expansions.

## Mutex Propagation for LA-MAPF

In this section, we describe a mutex-based symmetry-breaking technique for LA-MAPF. It first finds mutexes be-

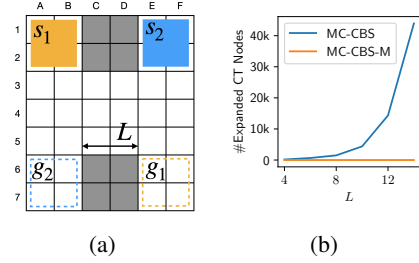


Figure 1: An example of a corridor conflict for two agents. Both agents are of  $2 \times 2$  square shapes, and we pick their top-left corners as reference points. (a) shows the start vertices  $s_1$  and  $s_2$  and the goal vertices  $g_1$  and  $g_2$  for these two agents. (b) shows the numbers of CT node expansions of two LA-MAPF algorithms for solving such problem instances as the corridor length  $L$  increases.

tween MDDs of a pair of agents using mutex propagation, and then it uses these mutexes to identify and automatically resolve cardinal conflicts.

Figure 1a shows an example of cardinal conflicts in LA-MAPF, which is similar to corridor symmetry in MAPF (Li et al. 2020; Lam et al. 2019). In this example, both agents are of size  $2 \times 2$ , and there is a “corridor” of width 3 and length  $L = 3$  in the middle of the map. In any optimal solution of this problem instance, either  $a_1$  or  $a_2$  needs to wait for the other agent to traverse the corridor. One needs to change the existing rule-based technique for corridor symmetries carefully so that it can be used here. In MAPF, corridor symmetries consider only corridors of width 1, which can be easily identified by finding vertices of degree 2. However, in LA-MAPF, corridor symmetries need to consider corridors of different widths depending on the sizes of the agents.

Mutex propagation takes the MDDs  $MDD_i^{l_i}$  and  $MDD_j^{l_j}$  as inputs (where  $l_i$  and  $l_j$  are determined by the algorithm and are not less than the individual minimum costs of agents  $a_i$  and  $a_j$ , respectively). For ease of presentation, we assume that  $l_i \leq l_j$ . We first find *initial mutexes*, which correspond to vertex and edge conflicts in LA-MAPF:

1. Two MDD nodes  $n_i \in MDD_i^{l_i}$  and  $n_j \in MDD_j^{l_j}$  are initial mutex iff  $n_i.level = n_j.level$  and agents  $a_i$  and  $a_j$  have a vertex conflict when they are at  $n_i.loc$  and  $n_j.loc$ , respectively, simultaneously.
2. Two MDD edges  $e_i = \langle n_i, n'_i \rangle$  and  $e_j = \langle n_j, n'_j \rangle$  with  $n_i, n'_i \in MDD_i^{l_i}$  and  $n_j, n'_j \in MDD_j^{l_j}$  are initial mutex iff  $n_i.level = n_j.level$  and agents  $a_i$  and  $a_j$  have an edge conflict when agent  $a_i$  moves from  $n_i.loc$  to  $n'_i.loc$  and agent  $a_j$  moves from  $n_j.loc$  to  $n'_j.loc$  simultaneously.

*Propagated mutexes* can be found using the following mutex-propagation rules:

1. *Forward propagation for MDD nodes:* Two MDD nodes  $n_i$  and  $n_j$  are propagated mutex iff neither  $n_i.level$  nor  $n_j.level$  is 0 and any MDD edge that points to  $n_i$  is either initial mutex or propagated mutex with any MDD edge that points to  $n_j$ .

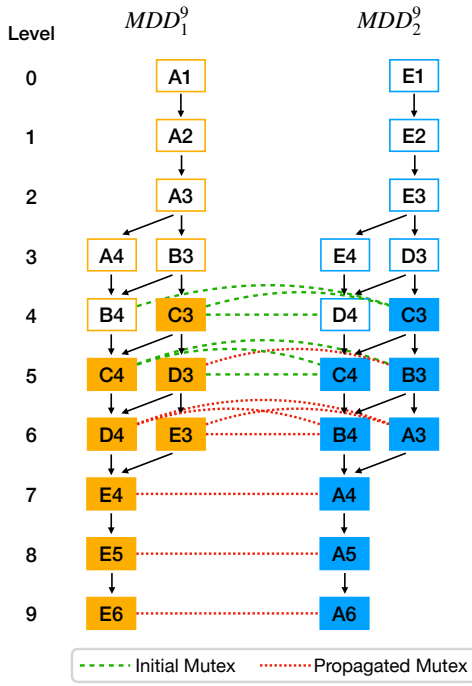


Figure 2: MDDs  $MDD_1^9$  and  $MDD_2^9$  for the problem instance in Figure 1a along with the mutexes between their MDD nodes. The labels inside the MDD nodes are the vertices of the agents. For ease of presentation, edge mutexes are not shown, and, for any pair of MDD nodes that are both initial and propagated mutex, only the initial mutex is shown. MDD nodes filled with color correspond to the constraint sets generated by the mutex-based technique.

2. *Forward propagation for MDD edges*: Two MDD edges  $\langle n_i, n'_i \rangle$  and  $\langle n_j, n'_j \rangle$  are propagated mutex iff MDD nodes  $n_i$  and  $n_j$  are either initial mutex or propagated mutex.

Two MDD nodes or two MDD edges are *mutex* iff they are initial mutex or propagated mutex. All mutexes between two MDDs can be found in time polynomial in the numbers of MDD nodes. Our definition of initial mutexes slightly differs from the one in (Zhang et al. 2020), which is specifically defined for vertex and edge conflicts in point-agent MAPF. Instead, we define it for general vertex and edge conflicts. By doing so, all theoretical properties of mutexes in (Zhang et al. 2020) are maintained because they are based on the conceptual equivalence of initial mutexes and conflicts.

Mutexes do not capture vertex conflicts that happen after agent  $a_i$  terminates because they are not propagated beyond level  $l_i$ . To handle cardinal conflicts caused by such vertex conflicts, Zhang et al. (2020) divided cardinal conflicts into two types and proposed an algorithm to identify and resolve each type of cardinal conflicts. To resolve a cardinal conflict between agents  $a_i$  and  $a_j$ , for each one of the conflicting agents, the algorithm identifies a set of MDD nodes in its MDD and converts each MDD node  $n$  into a vertex constraint on  $n.loc$  at timestep  $n.level$ . This results in two sets

of constraints  $C_i$  and  $C_j$ , one for each agent, that are used for CBS splitting. The two types of cardinal conflicts and their corresponding algorithms are:

1. *Pre-goal cardinal Conflicts (PCs)*: CBS identifies a PC between agent  $a_i$  and  $a_j$  iff the sink MDD node of  $MDD_i^{l_i}$  is mutex with all MDD nodes of  $MDD_j^{l_j}$  at level  $l_i$ . To resolve a PC, CBS uses two constraint sets  $C_i$  and  $C_j$  for agents  $a_i$  and  $a_j$ , respectively. Constraint set  $C_i$  contains the vertex constraints for every MDD node of  $MDD_i^{l_i}$  that is mutex with all MDD nodes of  $MDD_j^{l_j}$  at the same level. Similarly, constraint set  $C_j$  contains the vertex constraints for every MDD node of  $MDD_j^{l_j}$  that is mutex with all MDD nodes of  $MDD_i^{l_i}$  at the same level.
2. *After-goal cardinal Conflicts (ACs)*: CBS identifies an AC between agents  $a_i$  and  $a_j$  iff, for any MDD node  $n \in MDD_j^{l_j}$  at level  $l_i$  that is not mutex with the sink node of  $MDD_i^{l_i}$ , every path from  $n$  to the sink node of  $MDD_j^{l_j}$  traverses an MDD node  $n'$  such that agents  $a_i$  and  $a_j$  have a vertex conflict when they are at vertices  $g_i$  and  $n'.loc$  simultaneously, respectively. To resolve an AC, constraint set  $C_i$  contains a constraint that forces the path cost of agent  $a_i$  to be larger than  $l_i$ . Constraint set  $C_j$  contains the constraints for all MDD nodes of  $MDD_j^{l_j}$  at level  $l_i$  that are mutex with the sink MDD node of  $MDD_i^{l_i}$  and the constraints for all MDD nodes  $n' \in MDD_j^{l_j}$  such that  $n'.level > l_i$  and agents  $a_i$  and  $a_j$  have a vertex conflict when they are at vertices  $g_i$  and  $n'.loc$  simultaneously, respectively.

**Example 1.** Figure 2 shows MDDs  $MDD_1^9$  and  $MDD_2^9$  for the problem instance in Figure 1a. Green dashed lines indicate initial mutexes, which correspond to conflicts between agents  $a_1$  and  $a_2$ , and red dashed lines indicate propagated mutexes. A PC can be identified between these two MDDs because the sink node of  $MDD_1^9$  is mutex with all MDD nodes of  $MDD_2^9$  at level 9, that is, the sink node  $MDD_2^9$ . The MDD nodes that are used to generate the constraint sets are filled with color.

The mutex-based technique can generate different constraint sets for different choices of  $l_i$  and  $l_j$  as long as a cardinal conflict can be identified using  $MDD_i^{l_i}$  and  $MDD_j^{l_j}$ . Intuitively, larger values of  $l_i$  and  $l_j$  result in “stronger” constraints for CBS splitting. For example, the constraint sets in Example 1 will force agent  $a_1$  to take a path with a cost of 10 in one CT node and agent  $a_2$  to take a path with a cost of 10 in the other CT node, which is insufficient to resolve all conflicts between the agents. Zhang et al. (2020) proposed a greedy approach for determining the values of  $l_i$  and  $l_j$ , which we also use in our implementation. Due to the space limit, we skip the details of this approach.

For a cardinal conflict between agents  $a_i$  and  $a_j$ , let  $MDD_i^{l_i}$  and  $MDD_j^{l_j}$  denote the MDDs used for generating the constraint sets,  $l_i^*$  and  $l_j^*$  denote the individual minimum cost of agents  $a_i$  and  $a_j$ , and  $\delta_i$  and  $\delta_j$  denote  $l_i - l_i^*$  and  $l_j - l_j^*$ , respectively. The larger  $\delta_i$  and  $\delta_j$ , the more the path

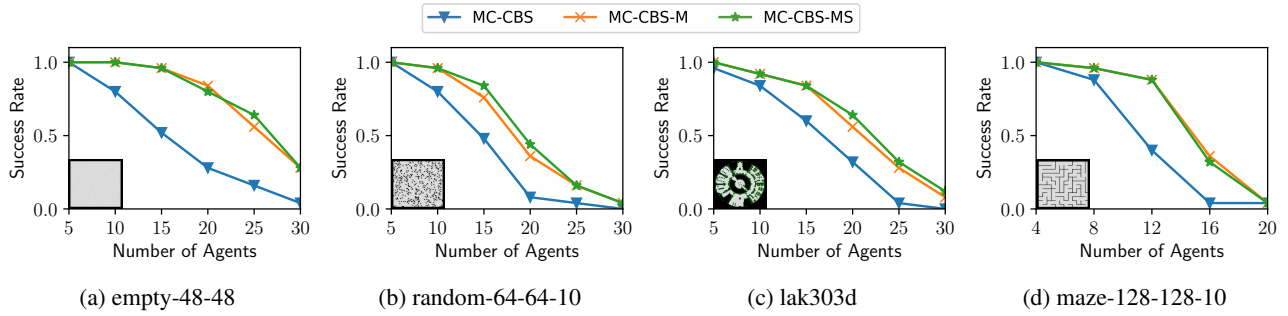


Figure 3: Success rates of various LA-MAPF solvers on each map with different numbers of agents.

costs of agents  $a_i$  and  $a_j$  need to increase in order to resolve the conflict. In some sense, larger values of  $\delta_i$  and  $\delta_j$  indicate that the conflict is more difficult to resolve and might be better resolved first. This motivates us to develop a new conflict selection rule based on  $\delta_i$  and  $\delta_j$ : When multiple cardinal conflicts are found in one CT node, we prefer to resolve the cardinal conflict with the largest  $\min(\delta_i, \delta_j)$  value next.

### Experimental Results

In this section, we compare different variants of MC-CBS, a state-of-the-art CBS-based solver for LA-MAPF. These variants are MC-CBS, MC-CBS-M, and MC-CBS-MS, where M denotes mutex-based symmetry breaking and S denotes the new conflict-selection rule. All MAPF solvers share the same codebase as much as possible. We chose four representative maps from the MAPF benchmark (Stern et al. 2019),<sup>1</sup> which are empty-48-48, random-64-64-10, lak303d, and maze-128-128-10. For each map, we generated 25 instances with randomly selected start and goal vertices for each agent. All agents are of square shape and size, varying from  $2 \times 2$  to  $3 \times 3$ . We ran all experiments on a MacBook Pro with 32GB of memory. The time limit for solving each LA-MAPF instance was five minutes.

Figure 3 shows the *success rate*, that is, the percentage of LA-MAPF instances that an algorithm solves within the time limit, for each map and different numbers of agents. In all four maps, the addition of mutex-based symmetry breaking improves the success rate. The improvement is large for empty-48-48. For instance, when the number of agents is 20, MC-CBS only solves 25% of the instances while both MC-CBS-M and MC-CBS-MS solve more than 75% of the instances. The new conflict-selection rule also slightly improves the success rate for empty-48-48, random-64-64-10, and lak303d.

Figure 4 shows the individual runtimes (in seconds) of MC-CBS and MC-CBS-MS for all maps and all numbers of agents. We use different colors to distinguish instances on different maps. There is no instance that MC-CBS solves but MC-CBS-MS does not solve within the time limit. For instances that both algorithms solve within 1 second, MC-CBS-MS is often slightly slower than MC-CBS due to the computational overhead of mutex reasoning. For more difficult instances, MC-CBS-MS solves most instances much

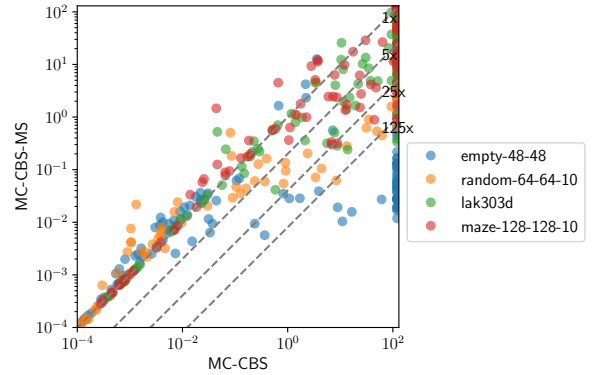


Figure 4: Runtimes of MC-CBS and MC-CBS-MS on all LA-MAPF instances. Each dot corresponds to an LA-MAPF instance, and its  $x$ -coordinate and  $y$ -coordinate correspond to the runtime (in seconds) of MC-CBS and MC-CBS-MS, respectively.

faster than MC-CBS. The improvement is large on some instances of empty-48-48, where the speedups are over  $125\times$ .

### Conclusion

In this paper, we showed that mutex-based symmetry-breaking techniques can be easily generalized to richer MAPF problems than the classical one, as we demonstrated for LA-MAPF. We also presented a mutex-based conflict-selection strategy. Our experimental results showed that our techniques significantly improve MC-CBS, a state-of-the-art optimal LA-MAPF algorithm, in terms of both success rate and runtime.

While our mutex-based technique can handle generalized vertex and edge conflicts, it still requires mutexes to connect pairs of MDD nodes or edges at only the same level and thus might not apply to problems like  $k$ -robust MAPF (Atzmon et al. 2018), where a conflict happens if an agent occupies a vertex that was occupied by another agent at most  $k$  timestep ago. Such conflicts can be modeled using a mutex between two MDD nodes on different levels. An interesting direction for future work is therefore to generalize mutex propagation and mutex-based symmetry-breaking techniques to mutexes between MDD nodes on different levels.

<sup>1</sup><https://movingai.com/benchmarks/mapf.html>

## Acknowledgments

The research at the University of Southern California was supported by the National Science Foundation (NSF) under grant numbers 1409987, 1724392, 1817189, 1837779, 1935712, and 2112533 as well as a gift from Amazon. The views and conclusions contained in this document are those of the authors and should not be interpreted as representing the official policies, either expressed or implied, of the sponsoring organizations, agencies, or the U.S. government.

## References

- Atzmon, D.; Stern, R.; Felner, A.; Wagner, G.; Barták, R.; and Zhou, N.-F. 2018. Robust Multi-Agent Path Finding. In *Annual Symposium on Combinatorial Search (SoCS)*, 2–9.
- Lam, E.; Bodic, P. L.; Harabor, D.; and Stuckey, P. J. 2019. Branch-and-Cut-and-Price for Multi-Agent Pathfinding. In *International Joint Conference on Artificial Intelligence (IJ-CAI)*, 1289–1296.
- Li, J.; Gange, G.; Harabor, D.; Stuckey, P. J.; Ma, H.; and Koenig, S. 2020. New Techniques for Pairwise Symmetry Breaking in Multi-Agent Path Finding. In *International Conference on Automated Planning and Scheduling (ICAPS)*, 193–201.
- Li, J.; Harabor, D.; Stuckey, P. J.; Ma, H.; and Koenig, S. 2019a. Symmetry-Breaking Constraints for Grid-Based Multi-Agent Path Finding. In *AAAI Conference on Artificial Intelligence (AAAI)*, 6087–6095.
- Li, J.; Surynek, P.; Felner, A.; Ma, H.; Kumar, T. S.; and Koenig, S. 2019b. Multi-Agent Path Finding for Large Agents. In *AAAI Conference on Artificial Intelligence (AAAI)*, 7627–7634.
- Ma, H.; Tovey, C.; Sharon, G.; Kumar, T. K. S.; and Koenig, S. 2016. Multi-Agent Path Finding with Payload Transfers and the Package-Exchange Robot-Routing problem. In *AAAI Conference on Artificial Intelligence (AAAI)*, 3166–3173.
- Morris, R.; Pasareanu, C. S.; Luckow, K.; Malik, W.; Ma, H.; Kumar, T. K. S.; and Koenig, S. 2016. Planning, Scheduling and Monitoring for Airport Surface Operations. In *AAAI-16 Workshop on Planning for Hybrid Systems*.
- Sharon, G.; Stern, R.; Felner, A.; and Sturtevant, N. R. 2015. Conflict-Based Search for Optimal Multi-Agent Pathfinding. *Artificial Intelligence*, 219: 40–66.
- Sharon, G.; Stern, R.; Goldenberg, M.; and Felner, A. 2013. The Increasing Cost Tree Search for Optimal Multi-Agent Pathfinding. *Artificial Intelligence*, 195: 470–495.
- Stern, R.; Sturtevant, N. R.; Atzmon, D.; Walker, T.; Li, J.; Cohen, L.; Ma, H.; Kumar, T. K. S.; Felner, A.; and Koenig, S. 2019. Multi-Agent Pathfinding: Definitions, Variants, and Benchmarks. In *Annual Symposium on Combinatorial Search (SoCS)*, 151–158.
- Walker, T. T.; Sturtevant, N. R.; Felner, A.; Zhang, H.; Li, J.; and Kumar, T. S. 2021. Conflict-Based Increasing Cost Search. In *International Conference on Automated Planning and Scheduling (ICAPS)*, 385–395.
- Wurman, P. R.; D’Andrea, R.; and Mountz, M. 2008. Coordinating Hundreds of Cooperative, Autonomous Vehicles in Warehouses. *AI Magazine*, 29(1): 9–20.
- Yu, J.; and LaValle, S. M. 2013. Structure and Intractability of Optimal Multi-Robot Path Planning on Graphs. In *AAAI Conference on Artificial Intelligence (AAAI)*, 1443–1449.
- Zhang, H.; Li, J.; Surynek, P.; Koenig, S.; and Kumar, T. K. S. 2020. Multi-Agent Path Finding with Mutex Propagation. In *International Conference on Automated Planning and Scheduling (ICAPS)*, 323–332.